

## Landscape-scale forest restoration decreases vulnerability to drought mortality under climate change in southwest USA ponderosa forest

Lisa A. McCauley <sup>a,\*</sup>, John.B. Bradford <sup>b</sup>, Marcos D. Robles <sup>a</sup>, Robert K. Shriver <sup>c</sup>, Travis J. Woolley <sup>a</sup>, Caitlin A. Andrews <sup>b</sup>

<sup>a</sup> The Nature Conservancy, Center for Science and Public Policy, 1510 E Ft Lowell Road, Tucson, AZ, USA

<sup>b</sup> U.S. Geological Survey, Southwest Biological Science Center, Flagstaff, AZ, USA

<sup>c</sup> University of Nevada, Department of Natural Resources and Environmental Science, Reno, NV, USA



### ARTICLE INFO

#### Keywords:

Climate change  
Drought mortality  
Forest restoration  
*Pinus ponderosa*  
southwestern USA

### ABSTRACT

Drought-induced tree mortality is predicted to increase in dry forests across the globe as future projections show hotter, drier climates. This could potentially result in large-scale tree die-offs, changes in species composition, and loss of forest ecosystem services, including carbon storage. While some studies have found that forest stands with greater basal areas (BA) have higher drought mortality, many have not evaluated the extent to which forests restored to lower densities via restoration activities affect drought mortality. The southwestern USA is particularly susceptible to tree mortality due to the predicted increases in temperature, drier soils, and forests with high density. Our objective was to evaluate how ponderosa pine mortality is expected to be influenced by the Four Forests Restoration Initiative (4FRI), a large-scale forest restoration effort ongoing in northern Arizona, USA, that will reduce stand BA by approximately 40%. Specifically, we modeled drought mortality in three time periods, one contemporary (1970–2010), and two future (2020–2059 and 2060–2099) under three restoration scenarios: no thinning, 4FRI thinning, and a BA reduction beyond the 4FRI plan (4FRI-intensive). We estimated mortality using 11 climate models under two emissions scenarios. Without thinning, our model predicted that by mid-century (2020–2059), changes in climate could increase annual ponderosa pine mortality rates by 45–57% over contemporary rates. However, with thinning, mid-century mortality was predicted to remain near or below contemporary rates and these rates are 31–35% (4FRI) and 46–51% (4FRI-intensive) less than the mid-century scenarios without thinning. Our study shows that while climate change is likely to increase tree mortality rates, large-scale forest restoration projects, such as 4FRI, have the potential to ameliorate the effects of climate change and keep mortality rates near contemporary levels for decades.

### 1. Introduction

Forests across the globe, particularly dry forests, are experiencing hotter, drier climates leading to increased tree mortality via drought (Allen et al., 2010; Anderegg et al., 2019; McDowell et al., 2016; Zhao and Running, 2010), higher fire risk (Dennison et al., 2014; Dillon et al., 2011), and larger and more frequent insect outbreaks (Allen and Breshears, 1998; Breshears et al., 2005). High tree mortality is predicted to change tree species composition, age structure, and forest ecosystem services, such as carbon storage (Allen and Breshears, 1998; Fettig et al., 2013; van Mantgem et al., 2009). Rising temperatures, longer droughts, and increased aridity predicted under climate change are expected to exacerbate factors and lead to higher tree mortality (McDowell et al.,

2016; van Mantgem et al., 2013; Williams et al., 2010). Trees in drought-prone areas like the southwestern USA, where forests are seasonally dry, are particularly susceptible to drought-related mortality due to higher temperature and drier soils projected by many climate models, some estimating 70–100% tree mortality (McDowell et al., 2016; Seager and Vecchi, 2010; Williams et al., 2013). Lower soil moisture availability combined with higher temperatures is referred to as “hot-drought” and may have the greatest impact on forests in the region (Bradford et al., 2022; Breshears et al., 2018; Choat et al., 2012). The effects of hot-droughts on trees can be direct, such as hydraulic failure or carbon starvation, or indirect, through increased susceptibility to pests and pathogens (Adams et al., 2017; Allen et al., 2015; Choat et al., 2012; McDowell et al., 2013). Given the accumulation of evidence of drought-

\* Corresponding author.

E-mail address: [lisa.mccauley@tnc.org](mailto:lisa.mccauley@tnc.org) (L.A. McCauley).

induced tree mortality, the long-term persistence of forest cover, especially in the southwestern USA, is uncertain.

In addition to the climatic triggers for tree mortality, high stand density contributes to heightened tree mortality (Bradford and Bell, 2017; McDowell et al., 2006; Young et al., 2017) but few studies have accounted for the effects of forest structure or forest management to reduce densities on water competition and subsequent drought mortality, particularly when predicting future mortality (Bradford et al., 2022). Globally, many forests have experienced increased tree density due to human alteration to the landscapes, some leading to higher tree mortality (Bigler et al., 2006; Heinrichs and Schmidt, 2009; Linares et al., 2009; Mantero et al., 2020). Dry forests in the western USA historically experienced frequent, low-intensity fires that thinned out seedlings and saplings and kept stand densities low. However, a history of fire suppression across forests has altered the forest structure and led to higher stand basal area (BA; a measure of density that accounts for size and number of trees in a stand; Covington and Moore, 1994; Fulé et al., 1997; Hagmann et al., 2021; Hessburg et al., 2019) than has been seen in the past, increasing competition among trees for available resources (Guarín and Taylor, 2005; Taylor, 2000; Taylor and Skinner, 2003). Higher BA has also been shown to increase the risk of large-scale insect outbreaks and the risk of severe wildfires, which contribute to higher mortality and are exacerbated by drought (Hurteau et al., 2014; McCauley et al., 2019; Raffa et al., 2008). Higher stand density, particularly when paired with hot-drought, will increase the likelihood of large-scale tree die-offs and could alter the distribution and ecosystems services provided by southwestern USA forests (Bradford and Bell, 2017; Das et al., 2011; Ruiz-Benito et al., 2013; Young et al., 2017).

Forest managers have few tools available to increase forest resistance to drought, but reduction of BA through restoration can reduce competition among trees for scarce water resources during a drought and improve post-drought recovery (Bottero et al., 2017). Reduction of forest density through mechanical thinning is a common practice to reduce fuel for wildfires, achieve wildlife habitat improvement, and protect urban areas (D'Amato et al., 2017). Reducing BA has also been shown to increase forest resistance to drought, e.g. decreasing tree mortality, increasing tree growth, and limiting insect-related mortality (Bottero et al., 2017; Bradford et al., 2022, 2020; Bradford and Bell, 2017; D'Amato et al., 2013; Gleason et al., 2017; McDowell et al., 2006; Restaino et al., 2019; Young et al., 2017). Recent attempts to increase the pace and scale of restoration include the Collaborative Forest Landscape Restoration Program, which has completed fuel reduction treatments on 3.8 million acres in US (USDA, Forest Service, 2020), the North Yuba Forest Partnership program (South Yuba River Citizens League, 2019), and projects to restore forests in the Rocky Mountains (Rocky Mountain Restoration Rocky Mountain Restoration Initiative, 2019). Large-scale restoration projects such as these present an opportunity to better understand the forest and edaphic settings and scales at which ecological restoration can ameliorate drought. A recent regional analysis of ponderosa pine forest densities and drought mortality characterized the drought-density interactions in a quantitative model that can be used to assess restoration benefits for minimizing mortality (Bradford et al., 2022). They suggested that a 50% reduction in BA in ponderosa forests could result in 20–80% reduction in mortality rates but no studies have evaluated the effect on mortality rates under climate change for planned density-reduction treatments in an ongoing, large-scale forest restoration.

The Four Forests Restoration Initiative (4FRI) is the largest forest restoration project currently being undertaken by the U.S. Forest Service and is part of the Collaborative Forest Landscape Restoration Program (CFLRP). The goal for 4FRI is to use science-based approaches to increase the pace and scale of forest restoration activities, via mechanical thinning and prescribed fire, to reduce risk from uncharacteristic wildfire and improve ecological and watershed health. This ongoing restoration project, and similar large-scale restoration efforts across western USA, present the opportunity to evaluate if restoration efforts primarily

aimed at reducing wildfire risk, can also reduce tree mortality rates under climate change.

The objective of this study was to estimate the effect of hot-drought on ponderosa pine (*Pinus ponderosa* subsp. *brachyptera* (Engelm. in Wislizenus)) mortality in northern Arizona and to evaluate the degree to which thinning treatments could reduce these effects in future climates. Specifically, we wanted to evaluate contemporary (1970–2010) ponderosa pine mortality rates in the study area using previously established drought-BA relationships (i.e. that stands with higher BA could be more vulnerable to drought; Bradford et al., 2022) and project the effects of thinning treatments and climate change, particularly hot-drought, on mortality rates in the future. We used desired-condition data from the 4FRI implementation plan to estimate, as closely as possible, the actual post-treatment basal areas expected in stands that will be thinned across the study area, as well as a more intensive thinning scenario. In comparison to no thinning scenarios, we hypothesized that scenarios with thinning treatments would lead to lower ponderosa pine mortality under climate change in the future.

## 2. Methods

The study area was the first phase of the Four Forest Restoration Initiative (4FRI) and covers ~ 400,000 ha in the Coconino and Kaibab National forests in northern Arizona, USA (Fig. 1). This landscape is dominated by ponderosa pine, ponderosa pine and oak, and intermixed with dry and wet mixed conifer forest types. The elevation ranges from 1,780 to 3,850 m with a mean elevation of 2,190 m. Within the study area, we evaluated mortality on 4FRI stands with dominant ponderosa pine vegetation (greater than 70% BA) for which a mechanical thinning treatment was prescribed, according to the 4FRI implementation plan. This included 6,811 stands covering ~ 137,200 ha (Fig. 1).

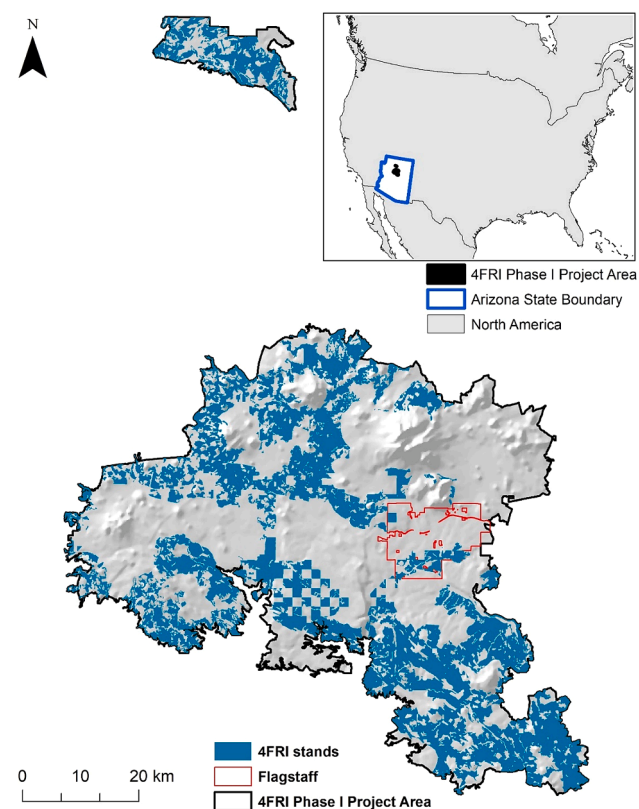


**Fig. 1.** Locations of ponderosa pine stands that were thinned within the Phase 1 of the Four Forests Restoration Initiative (4FRI) boundary in northern Arizona, USA.

## 2.1. Scenarios

We examined mortality in each stand in three time periods: contemporary (1970–2010); mid-century (2020–2059); and late-century (2060–2099). Additionally, we evaluated mortality in three forest restoration treatment scenarios: no thinning (all time periods BA in each stand was maintained as estimated in 2010 by the U.S. Forest Service), 4FRI (future BA for each stand was maintained at the proposed levels in the 4FRI implementation plan); and 4FRI-Intensive (hereafter 4FRI-I; future BA for each stand was maintained at a reduction meant to represent historical BA). BA averages for each scenario were: no-thinning – 29.5 m<sup>2</sup>/ha +/- 8.4 (sd); 4FRI – 17.3 m<sup>2</sup>/ha +/- 4.6 (sd); and 4FRI-I – 9.7 m<sup>2</sup>/ha +/- 2.6 (sd; Fig. 2; additional metrics in Table A.1).

Contemporary BA (no thinning scenario) was calculated from U.S. Forest Service Common Stand Exam Inventory data and 4FRI BA was obtained from desired condition data for the 4FRI project landscape acquired from U.S. Forest Service (unpublished data). The 4FRI prescriptions varied across the landscape, with an average BA reduction of ~ 40%, and considered existing tree density, desired canopy openness, and age and size class diversity to meet management objectives related to wildfire risk reduction, watershed health, and wildlife. 4FRI-I was not a planned restoration scenario, so BA for the 4FRI-I scenario was calculated by comparing the median of historical BA values from published studies in the region (Table 6; Reynolds et al., 2013) to the median of the 4FRI treatment with the greatest BA reduction. The comparison suggested that taking a further BA reduction from the 4FRI data of 0.56, would better represent historical range of variability. Our estimates of future BA assume that BA will be maintained at treatment levels and we do not include demographic processes that allow for recruitment or growth. This assumption is consistent with 4FRI implementation plans where additional restoration, often in the form of prescribed fire, will be used to maintain initial treatment BA levels.

## 2.2. Covariates

To calculate covariates representing hot-drought, we used the SOILWAT2 ecosystem water balance model (Schlaepfer and Murphy,

2018). SOILWAT2 is a daily time-step, multiple soil-layer, process-based, simulation model of ecosystem water balance, that models stand-specific interactions between soil, vegetation, and climate (Bradford et al., 2014). Vegetation in SOILWAT2 is represented by the fraction of each plant functional type (PFT), and monthly total biomass, monthly foliar biomass, and leaf area index (LAI) conversion for each PFT. Biomass was determined from plot data and allometric equations in Jenkins et al. (2003). LAI and the fraction of grass were determined from Flathers et al. (2016). Because we wanted to evaluate the impact of basal area on mortality in our statistical models, we eliminated the influence of basal area on estimated drought conditions in the SOILWAT2 modeling by using a constant value for basal area at each stand in SOILWAT2 and set to the median value (20 m<sup>2</sup>/ha) across all plots examined. Soil texture was extracted for each stand from the ISRIC soils 250 m v5 (Hengl et al., 2017) data in 3 soil profiles at depths of 0–15 cm, 15–60 cm, and 60–200 cm. Maximum soil depth was also extracted for each stand from the ISRIC dataset. We evaluated SOILWAT2 output using the rSFSW2 R package (Schlaepfer and Andrews, 2018) and calculated soil water availability (SWA) as the amount of water that could be extracted from the soil profile before all soil layers reached a soil water potential of – 3.0 MPa, an estimate of the lowest water potential at which ponderosa pine can extract water (Kolb et al., 1998).

Contemporary (1970–2010) daily temperature and precipitation input climate data for SOILWAT2 and temperature covariates were obtained from Livneh et al. (2013). Future input temperature and precipitation were extracted as monthly time-series for two time periods, 2020–2059 (mid-century) and 2060–2099 (late-century) from one-half degree downscaled and bias-corrected data from the fifth phase of the Climate Model Intercomparison Project (CMIP5; Maurer et al., 2007; Taylor et al., 2012). To model more realistic spatial and temporal variation for the future climate data, the future CMIP5 data was combined with the contemporary data using a hybrid-delta downscaling method to obtain future daily data at 1/16th degree resolution (Dickerson-Lange and Mitchell, 2014; Hamlet et al., 2010; Tohver et al., 2014). Eleven GCMs were selected (Knutti and Sedláček, 2013; Rupp et al., 2013) and included CanESM2, CESM1-CAM, CNRM-CM, CSIRO-Mk3-6-0, FGOALS-g2, FGOALS-s2, GISS-E2-R, HadGEM2-ES, inmcm4, IPSL-CM, and MIROCESM. GCM data from Representative

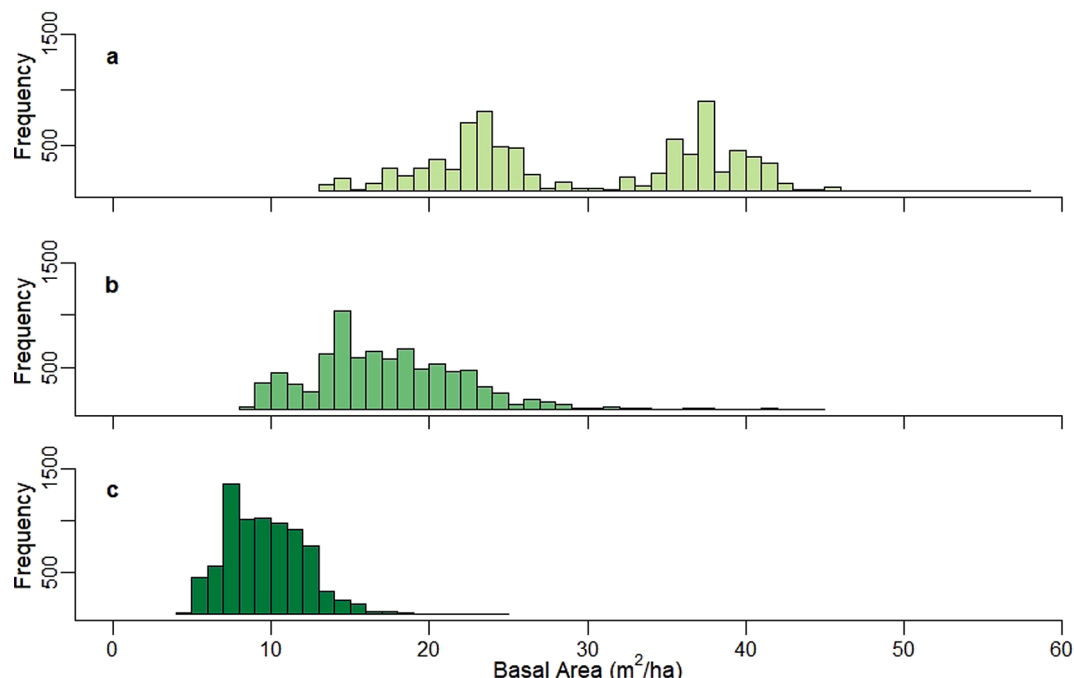


**Fig. 2.** Basal areas of all modeled stands within the Four Forests Restoration Initiative (4FRI) under a) no thinning scenario, b) 4FRI thinning scenario, and c) 4FRI-Intensive thinning scenario.

Concentration Pathways (RCPs) 4.5 and 8.5 were used. Variations in GCMs are displayed by showing the minimum, maximum, and median GCM at each stand for each covariate and in the predicted mortality. Spatial patterns in maps are displayed using only the median GCM at each stand and for RCP 4.5.

For our tree mortality models, we used coefficients and covariates from a previously established model in Bradford et al. (2022). In the previously established model, ponderosa pine decadal survival was estimated from Forest Inventory and Analysis (FIA) plots across the western U.S. from 2000 to 2017. The model we use here was the top performing model from a list of competing models to explain ponderosa pine mortality across all western U.S. sites, including sites in our study area. All variables in the original model were tested for multicollinearity and highly correlated variables were removed. Posterior predictive checks indicated good agreement between mean model predictions and observed data ( $p = 0.53$ ). Spatial random effects were included in the original model to account for the impact of spatial autocorrelation on parameter inference (See Bradford et al., 2022 for full description; Banerjee et al., 2008). Observed values for covariates from our study region are consistent with the observed values from the full region (Table A.2). The covariates used are listed and defined in Table 1.

We used quadratic mean diameter (QMD) from each stand for tree size from the U.S. Forest Service 4FRI data provided for No Thinning and

$$S = QMD + BA + \text{TEMP}_{\text{MEAN}} + \text{SWA}_{\text{MEAN}} + \text{TEMP}_{7\text{YMAX}} + \text{SWA}_{8\text{YMIN}} + \text{SWA}_{3\text{YMAX}} + \text{TEMP}_{\text{MEAN}} * BA + \text{SWA}_{\text{MEAN}} * BA + \text{TEMP}_{7\text{YMAX}} * BA + \text{SWA}_{8\text{YMIN}} * BA$$

4FRI scenarios. Because 4FRI-I was not a scenario run by the U.S. Forest Service, the relationship between decreased BA and increased QMD in 4FRI scenario (on average 39% less BA led to 37% greater QMD) was extrapolated to the increased reduction in BA for the 4FRI-I scenario (on average 66% reduction in BA for the 4FRI-I scenario was extrapolated to a 63% increase in QMD). The average QMD was: 23.6 cm for the no thinning treatment; 32.0 cm for the 4FRI; and 38.5 cm for 4FRI-I scenarios.

### 2.3. Mortality model

Mortality was estimated for each selected stand and within each scenario/time-period combination using coefficients from the previously established model from Bradford et al. (2022). Survival probability for the 10 years between FIA measurements was modeled following Shriner et al. (2021) as:

**Table 1**

Covariate abbreviations and descriptions for the covariates used in the mortality model.

Covariate Abbreviation	Covariate Description
QMD	Quadratic Mean Diameter for stand
BA	Sum of tree cross-sectional basal area at 1.37 m height ( $\text{m}^2\text{ha}^{-1}$ )
SWA <sub>MEAN</sub>	Mean April-September soil water availability from 1970 to 2010 (cm)
TEMP <sub>MEAN</sub>	Average April-September air temperature from 1970 to 2010 (°C)
SWA <sub>8YMIN</sub>	Lowest April-September soil water availability during a consecutive 8-year period in each decade (cm) subtracted from SWA <sub>MEAN</sub>
TEMP <sub>7YMAX</sub>	Highest April-September temperature during a consecutive 7-year period in each decade (°C) subtracted from TEMP <sub>MEAN</sub>
SWA <sub>3YMAX</sub>	Highest April-September soil water availability during a consecutive 3-year period in each decade (cm) subtracted from the SWA <sub>MEAN</sub>

$$p_{i,t+1} \sim \text{Bern}(s_{i,t})$$

$$\text{logit}(s_{i,t}) = \alpha z_{i,t} + \mathbf{X}_{d[i]} \mathbf{b} + \omega_{d[i]}$$

where  $s_{i,t}$  is the probability of survival for individual  $i$  from  $t$  to  $t + 1$ ,  $z_{i,t}$  is the diameter of tree  $i$  in the first census ( $t$ ),  $\alpha$  is a regression coefficient for the impact of tree size (QMD) on survival that allows tree size to influence survival rate,  $\mathbf{b}$  is a vector of regression coefficients (see list of coefficients below) for environmental conditions and basal area terms,  $\mathbf{X}_{d[i]}$  is a design matrix including all plot-covariates and an intercept for individual  $i$ , and  $\omega_{d[i]}$  is a plot-specific spatial random effect for each individual  $i$ . Spatial random effects were used to account for spatially autocorrelated residual error not accounted for by covariates and were not carried forward to projections of mortality in the 4FRI regions during contemporary and future time periods (see below).

Covariates included BA, mean temperature (TEMP<sub>MEAN</sub>; and its interaction with BA), mean soil water availability (SWA<sub>MEAN</sub>; and its interaction with BA), 7-year high temperature anomaly (TEMP<sub>7YMAX</sub>; and its interaction with BA), 8-year low soil moisture anomaly (SWA<sub>8YMIN</sub>; and its interaction with BA), and high 3-year high soil moisture anomaly (SWA<sub>3YMAX</sub>). The final model covariate structure, omitting covariate parameters for clarity, was:

Mean and standard deviation of coefficients from this model are included in Table A.2. The model was fit using Hamiltonian Monte Carlo (HMC) in Stan (Stan Development Team, 2020) with 2 chains, 5000 iterations each, 2500 for warmup. Parameter convergence was monitored with convergence statistics (R-hat; Gelman et al., 2013). Decadal survival was converted to annualized mortality.

To predict survival in our stands from the above model, coefficients from all 5,000 iterations were used and averaged across iterations. Climate means and anomalies were calculated for each decade and used to calculate decadal survival. Covariates in our model were scaled against the means and standard deviations of the covariates in the original model from Bradford et al (2022). We converted average decadal survival to annual mortality for presentation purposes using the formula  $M = 1 - S^{(1/10)}$ , where  $S$  = average decadal survival rates and  $M$  = annual mortality rates. Due to the difficulty in predicting the spatial random effects in new locations and into the future climates, we did not include them in our models.

To avoid non-linear averaging that would occur if we calculated differences between scenarios/time periods using posterior averages, we calculated the differences between GCMs assuming a fixed parameter set, and iteratively drawing parameter sets from the posterior distribution. We then averaged differences in GCM across all the iterations and used the GCM with the median difference to calculate percent changes.

A gridded soils data product, ISRIC 250 m (Hengl et al., 2017), was used as input into SOILWAT2 to match the soil inputs from the original model (Bradford et al., 2022). A more detailed, field-based soils data set from the U.S. Forest Service (U.S. Department of Agriculture, Forest Service, 1995, hereafter USFS soils data; 1991) has been used in previous studies in the region (Bradford et al., 2020; McCauley et al., 2019) and may likely be a more realistic estimate of soil textures and depths. However, the USFS soils data was not available throughout the geographic extent of the original model (in which the range of ponderosa pine was used to capture a larger range of variability), so ISRIC was used. When we compared both ISRIC and USFS soils data for the

study area, we found that the ISRIC data product overestimated the depth of soils compared to the USFS soils data (Fig. A.1). Accordingly, when the USFS soils data (with shallower depths) were used in SOIL-WAT2, the estimated SWA found the stands to be unusually drier (more than 2 standard deviations drier) than with the ISRIC soils data. Because the ISRIC product was used in the original models, we continued using it in our mortality models and all results presented in the main paper were from SWA calculated with these data. Nevertheless, we also ran the survival prediction models with the USFS soils data to conduct a sensitivity analysis to see if mortality outcomes varied in a systematic way based on soils data; these results are summarized below and presented in Figs. A.1 and A.2.

### 3. Results

#### 3.1. Temperature anomaly projections

All GCMs predict an increase in the 7-year growing season temperature anomalies with the greatest increases in the 2060–2099 time

period and in RCP 8.5 (Fig. 3). The mean temperature anomaly for 1970–2010 was 0.12 °C, indicating that the hottest consecutive 7 years in each decade were, on average, 0.12 °C hotter than the mean temperature from 1970 to 2010. Compared to the contemporary reference period (1970–2010), the mean 7-year maximum temperature anomaly across stands for the median GCM for RCP 4.5 was 2.3 °C for the 2020–2059 time period and 3.4 °C for the 2060–2099 time period. The average for the minimum GCM at each stand and average for the maximum GCM at each stand for the same RCP, hereafter GCM range, was 1.2–3.3 °C for 2020–2059 and 2.4–5.8 °C for 2060–2099 (Fig. 3). For RCP 8.5, the median GCM average across stands was predicted to be 2.5 °C (GCM range: 1.5–3.2 °C) and 5.2 °C (GCM range: 2.5–7.4 °C) for the 2020–2059 and 2060–2099 time periods, respectively (Fig. 3).

#### 3.2. Soil water anomaly projections

GCMs varied on the direction and magnitude of the soil water availability (SWA) drought anomalies with some predicting the driest consecutive 8-years each decade had lower SWA than the overall

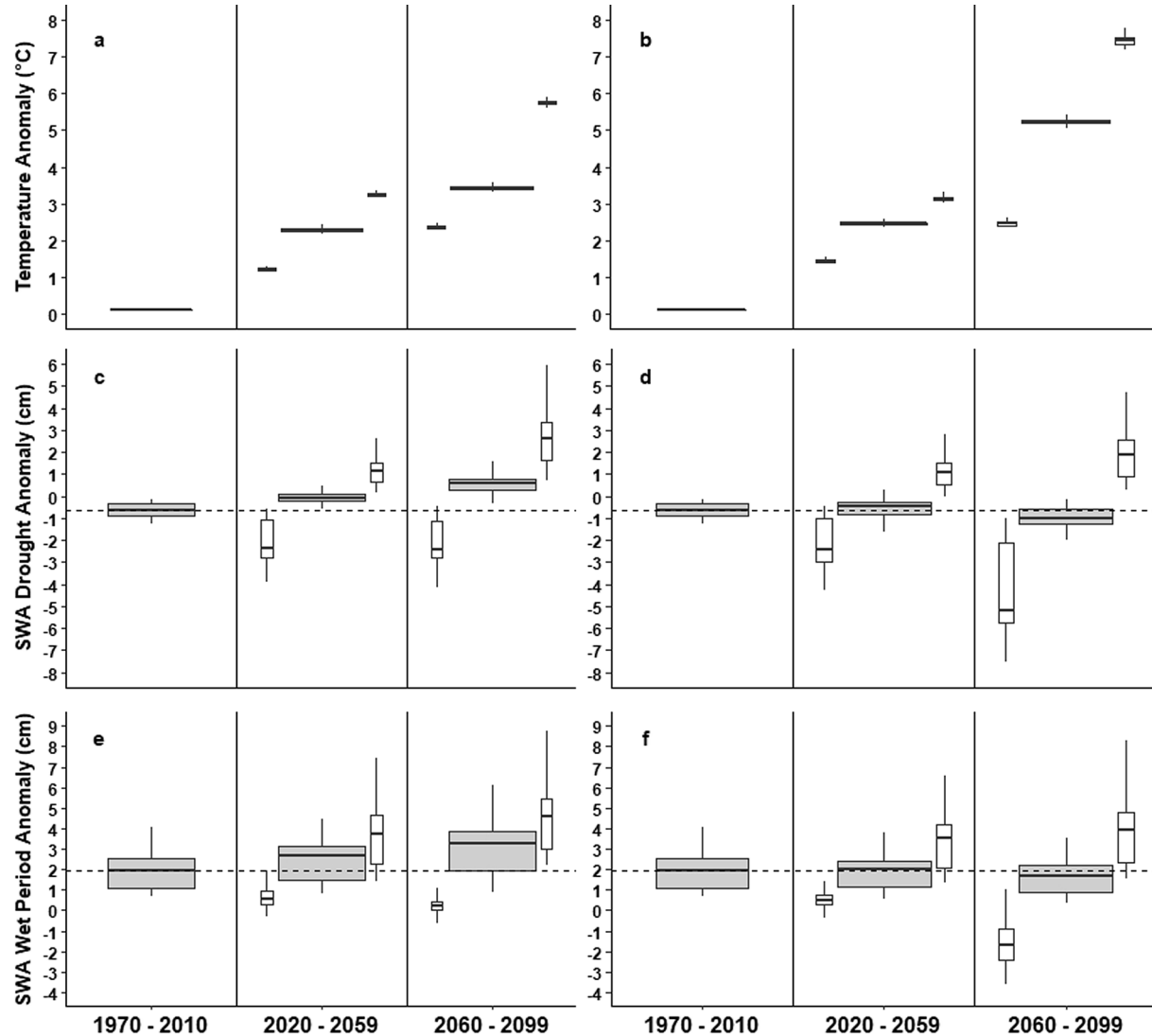


**Fig. 3.** Distributions of climate anomalies from the three time periods for: a) 7-year temperature anomaly for RCP 4.5; b) 7-year temperature anomaly for RCP 8.5; c) 8-year drought anomaly for RCP 4.5; d) 8-year drought anomaly for RCP 8.5; e) 3-year SWA wet period anomaly for RCP 4.5; and f) 3-year SWA wet period anomaly for RCP 8.5. The wider boxes represent the range in values for the median GCM at each stand and the thinner boxes to the left and right of the wider boxes represent the range in values from the minimum and maximum GCMs at each stand, respectively. The dashed lines depict the median anomaly for the 1970–2010 time period. Soil water availability (SWA) is the amount of water in cm that could be extracted from the soil profile before all soil layers reached a soil water potential of  $-3.0 \text{ MPa}$ .

contemporary average and some predicting the opposite (Fig. 3). The 1970–2010 average SWA drought anomaly was −0.63 cm. The SWA drought anomaly for the median GCM for RCP 4.5 was −0.04 cm (GCM range: −2.1–1.12 cm) and 0.56 cm (GCM range: −2.1–2.6 cm) for the 2020–2059 and 2060–2099 time periods, respectively (Fig. 3). For RCP 8.5, the SWA drought anomaly for the median GCM for the 2020–2059 time periods was −0.57 cm (GCM range: −2.13–1.06 cm) and for the 2060–2099 time period was −0.96 cm (GCM range: −4.25–1.78 cm).

The wet period SWA anomaly, which is calculated as the difference between the wettest consecutive 3-years in each decade and the mean SWA from 1970 to 2010, showed similar patterns to the SWA drought anomaly (Fig. 3). The contemporary wet period SWA anomaly for 1970–2010 was 1.84 cm. The median GCM in each stand for RCP 4.5 in the 2020–2059 time period had an average wet period anomaly of 2.4 cm (GCM range: 0.61–3.53 cm) and in the 2060–2099 time period averaged 2.98 cm (GCM range: 0.23–4.37 cm; Fig. 3). For RCP 8.5, the median GCM in each stand had an average wet period anomaly of 1.81 cm (GCM range: 0.53–3.22 cm) and 1.59 cm (GCM range: −1.69–3.68 cm) for the 2020–259 and 2060–2099 time periods, respectively (Fig. 3).

### 3.3. Mortality projections

#### 3.3.1. No thinning

We estimated median annual mortality in the contemporary period (1970–2010) at 1.0% and, without thinning, predicted an increase to an average of a 1.4% mortality rate in the 2020–2059 time period under RCP 4.5 (GCM range: 1.2–1.5%) or a 1.5% mortality rate under RCP 8.5 (GCM range: 1.3–1.7%) (Fig. 4; Table A.3). The median differences between GCM projections for the 2020–2059 time period and contemporary mortality estimated a 45% and 57% increase in mortality for RCP 4.5 and RCP 8.5, respectively. By the 2060–2099 time period, without thinning, mortality was estimated at 1.7% (GCM range: 1.4–1.9%) for RCP 4.5 or to a 2.4% mortality rate (GCM range: 1.8–3.9%) for RCP 8.5 (Fig. 4; Table A.3). The median difference between GCM projections for

the 2060–2099 time period and contemporary mortality estimated a 78% and 169% increase in mortality for RCP 4.5 and RCP 8.5, respectively. Please note that our calculation of differences between scenarios/time periods based on differences between individual GCMs (see methods) the percent change values reported here may differ slightly from differences between scenarios/time period calculated based on GCM median mortality rates.

#### 3.3.2. 4FRI

Under 4FRI thinning scenario, 2020–2059 mortality was predicted to be nearly the same as the contemporary mortality rate, 0.97% for 4FRI (GCM range: 0.6–1.2%) RCP 4.5 and 1.1% (GCM range 0.8–1.4%) for RCP 8.5 (Fig. 4; Table A.3). When comparing the 2020–2059 4FRI scenario to the same time period but without thinning, we found that 4FRI could reduce mortality rates by 35% in RCP 4.5 and by 31% in RCP 8.5. For the 2060–2099 time period, with 4FRI thinning, mortality rates were predicted to be 1.3% (GCM range: 0.9–1.8%) and 2.4% (GCM range: 1.5–4.4%) under RCP 4.5 and RCP 8.5, respectively. (Fig. 4; Table A.3). These rates represent a 34% and 154% (RCP 8.5) increase in 4FRI mortality rates over contemporary rates, and a 26% (RCP 4.5) and 6% (RCP 8.5) decrease in 4FRI mortality rates when compared to the same time period but with no thinning.

#### 3.3.3. 4FRI-I

To evaluate the influence of thinning intensity on drought mitigation, we found that generally, predicted mortality was lowest in 4FRI-I scenario. By 2020–2059, the increased rate of thinning in the 4FRI-I scenario decreased mortality from the 1.0% found in the contemporary period to 0.8% mortality rate (GCM range: 0.5–1.5%) in RCP 4.5 and 0.9% mortality rate (GCM range: 0.6–1.7%) in RCP 8.5 (Fig. 4; Table A.3). The 4FRI-I scenario reduced mortality rates by 51% and 46% in 2020–2059 compared to the same time period with no thinning in RCP 4.5 and RCP 8.5, respectively. However, by the late-century time period, mortality increased in the 4FRI-I scenario, especially in RCP 8.5.

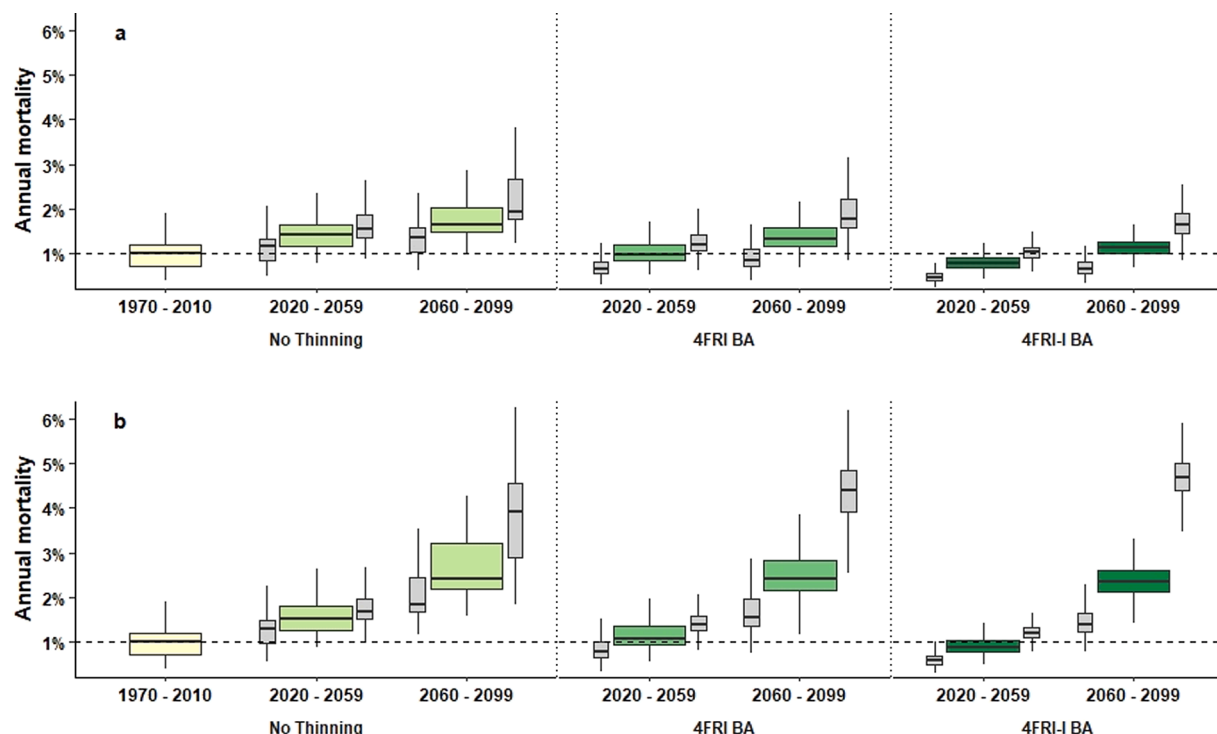


**Fig. 4.** Distributions of annual mortality for all scenarios and time periods in a) RCP 4.5 and b) RCP 8.5. The wider, green boxes represent the distribution of values from the median GCM and the thinner, grey boxes to the left and right of the wider boxes represent the range in values from the minimum and maximum GCMs, respectively. The dashed line represents the median value for annual mortality in the contemporary period (1970–2010). (For interpretation of the references to colour in this figure legend, the reader is referred to the web version of this article.)

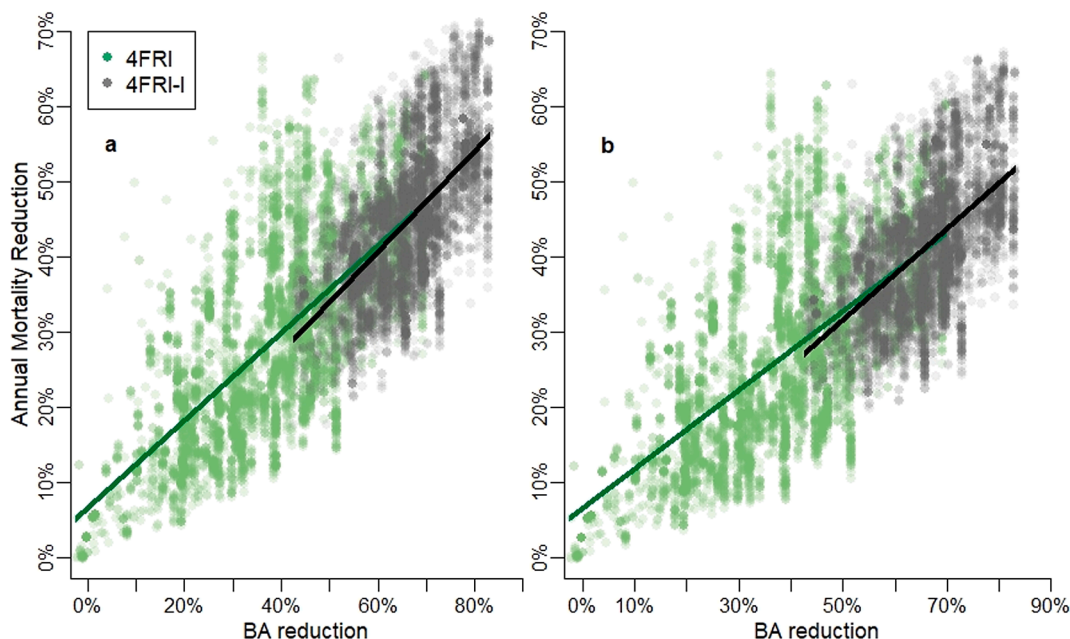


**Fig. 5.** Relationship between the percent reduction in annual mortality and the percent reduction in basal area (BA) for the mid-century time period (2020–2059) for a) RCP 4.5 and b) RCP 8.5. The BA reduction from the no thinning scenario to the 4FRI scenario is shown in green and the BA reduction from the no thinning scenario to the 4FRI-Intensive scenario is shown in blue. The colored lines represent the linear relationship between percent reduction in mortality and percent reduction in BA for each scenario. (For interpretation of the references to colour in this figure legend, the reader is referred to the web version of this article.)

We found mortality in RCP 4.5 for 2060–2099 to be 1.1% (GCM range: 0.7–1.7%) and 2.4% (GCM range: 1.4–4.7%; Fig. 4; Table A.3) in RCP 8.5. For RCP 4.5, this is a reduction of 39% over the same time period with no thinning. But in RCP 8.5, there is only a 9% reduction over the same time period with no thinning.

We identified two relationships that are useful for understanding variability in mortality patterns among stands. First, for the mid-century period (2020–2059), the reduction in drought mortality was proportionate to thinning intensity, with the highest reductions in mortality predicted to occur in stands with the highest thinning intensity (Fig. 5). Second, we found significant spatial heterogeneity in drought mortality across the study area, which was driven by both input soil and climate conditions, as well as by variation among stands in the treatment prescriptions (e.g. variation in target BA and tree size) defined by 4FRI (Fig. 6).

Mortality projections using USFS soils data indicate a similar pattern of mortality across scenarios as the gridded soils data, showing that thinning treatments reduced mortality (Fig. A.2). However, the USFS soils data, with shallower depths, produced SWA values that were substantially lower than the gridded soils data and thus, higher mortality rates overall.

#### 4. Discussion

Models developed in this study predict that changing climate conditions will increase tree mortality rates in the 4FRI landscape by 45–57% by mid-century without thinning. However, our results suggest that large-scale forest restoration projects that reduce tree density, such as 4FRI, have the potential to ameliorate the effects of climate change and keep mortality rates low for decades. Our contemporary mortality rates, around 1%, were consistent with other studies from the region (Bradford and Bell, 2017; van Mantgem et al., 2009). We found that under RCP 4.5 and RCP 8.5 scenarios, mid-century (2020–2059), 4FRI ecological restoration could sustain mortality rates near or below contemporary rates and could have 31–35% lower mortality rates when compared to the same time period with no thinning. We also found that density reductions beyond those planned by 4FRI and meant to

represent the historical range of variation in the region could have 46–51% lower mortality rates when compared to the same time period with no thinning. Large-scale tree mortality due to climate change has been predicted (Allen et al., 2010; Choat et al., 2012; McDowell et al., 2016), but our results suggest that forest restoration via ecological thinning provides an opportunity to enhance forest stand resistance to hot drought. Other studies have shown that hot drought and higher tree density can increase mortality (Allen et al., 2010; Bradford et al., 2022; Bradford and Bell, 2017; McDowell et al., 2006; Young et al., 2017) and here we applied those concepts to a specific, ongoing restoration effort and included modeling future hot drought in these locations with a water balance model to assess the influence of soil moisture.

Our model utilized relationships found from across the range of ponderosa pine in the western U.S. and considered multi-year temperature and drought anomalies, as well as wet periods that may have mitigated drought effects. Including these anomalies with tree density and their interactions, indicates that competition for resources (e.g. soil moisture) is a dominant influence in tree mortality and will likely have greater influence as hot droughts become more prevalent with future climate conditions (Luo and Chen, 2013, 2011). Reducing basal areas can reduce the stress trees experience as temperature rises and soil moisture declines by lowering the competition for resources. Our study did not simulate post-treatment tree growth or demography, keeping the treatment BA consistent into the future, following the implementation plan for 4FRI which will use periodic prescribed fire to maintain treatments. However, if BA levels do not remain consistent, trees will likely grow faster due to increased access to resources made available by thinning (Bradford et al., 2020) and the effects of the thinning could diminish in time as competition for resources increases again (Sohn et al., 2016).

Without thinning, our results suggest that ponderosa pine mortality will likely increase and could lead to substantial widespread tree mortality and potentially a loss of forest cover in the region. Trees that died from insect mortality were not specifically excluded from the original model used to develop the relationships in our model and thus, we cannot say whether the mortality represented in our models were caused by drought alone or if drought predisposed the trees to insect mortality

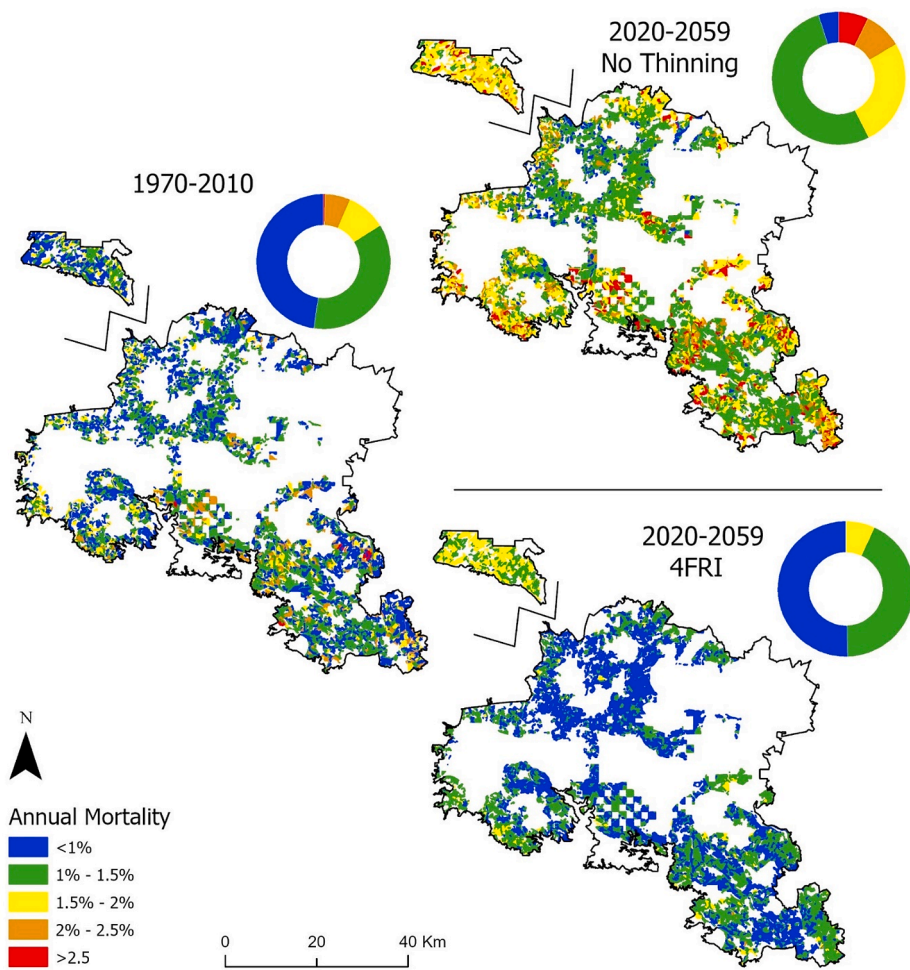


**Fig. 6.** Spatial distribution of the annual mortality across stands in the contemporary time period and the no thinning scenario and the 4FRI scenario in the 2020–259 time period, RCP 4.5. The donut plots represent the proportion of stands in each category of annual mortality. The lines between polygons depict that the northern portion of the landscape has been moved closer to the main portion of the landscape for display purposes.

(Ganey and Vojta, 2011). Insect mortality is likely to intensify with climate change (Bentz et al., 2010; Raffa et al., 2008; Williams and Liebhold, 2002) and will likely be a greater factor in tree mortality in this region than in the past. Our model did not include tree mortality from wildfire, but other studies have suggested that wildfire intensity will increase with climate change and contribute to even higher tree mortality (Hurteau et al., 2014; McCauley et al., 2019). Widespread tree die-off from drought, insects, and wildfire may occur at faster rates than tree growth and recruitment, decreasing the ability of forests to recover (Allen et al., 2015).

Few strategies exist for managers to increase forest resistance and limit the potential loss of forest cover, especially under future climate change, but our results suggest that forest restoration could accomplish this. In dry, fire-prone forests, restoration often includes moving toward historical stand structures and fire regimes. The goal of forest restoration often includes reducing wildfire risk, improving wildlife habitat, and restoring forest structure, function, and processes (U.S. Department of Agriculture, Forest Service, 2013). Maintaining dry forest cover is important because the forests provide ecosystem services like carbon storage, nutrient cycling, and hydrologic regulation as well as have cultural and recreational value (Breshears et al., 2011). A series of complementary studies have demonstrated the additional co-benefits associated the 4FRI restoration program, minimizing growth vulnerability (Bradford et al., 2020), increasing water supply (Robles et al., 2014), and stabilizing carbon (McCauley et al., 2019). The results from this study show the additional restoration benefit of increased forest

stand resistance to drought under future climate change. While our study evaluated the mortality reductions across individual stands, the cumulative effect of restoration at the landscape scale could have additional hydrologic benefits that would be likely to improve survival. Management to reduce tree densities may be a viable strategy in the coming decades to improve forest resistance and prevent large-scale die offs if restoration is implemented at the broadest scale feasible.

Limitations to our models include the ability of the regional model to predict into new spatial and temporal conditions, including the thinning scenarios modeled. While the observed values for covariates from our study region are consistent with the observed values from the full region, the thinning scenarios could potentially represent combinations of BA by climate conditions that weren't well represented in the regional model. The regional model from contemporary time periods doesn't represent the novel conditions expected during late-century time-period, especially in RCP 8.5. The temperature anomalies in late-century 2060–2099 time period are outside the range of temperature anomalies on which the mortality model was developed (Fig. 3; Bradford et al., 2022). Due to the lifespan of ponderosa pine, we assumed many trees that occur in the future time periods would have been recruited in contemporary climates. We calculated our anomalies to reflect this by subtracting the future temperatures from the contemporary means, leading to large temperature anomalies by the late century. Contemporary temperature anomalies in our study averaged 0.12 °C and considering the range of historical variation, anomalies from the mid-century time period, while higher than the contemporary anomalies,

may be reasonable. But temperature anomalies in the late century range to above 5° and the maximum GCMs in RCP 8.5 average 7.4°. Thus, relationships developed from those temperature anomalies are limited, as are our insights into the effect of BA reduction on mortality using those projections. As it is generally unknown, we also did not include the species' ability to adapt or acclimate to these future conditions. Additionally, although we considered a suite of climate models, near-term climate projections of both SWA and temperature are inherently more reliable than long-term, when RCPs and GCMs diverge from each other more (Briley et al., 2021). Given that planning windows for forest managers typically span 10–20 years, mid-century predictions are likely more relevant and are consistent with conclusion that a reduction in BA will reduce ponderosa pine mortality. The differences between RCP 4.5 and RCP 8.5, combined with the higher confidence in the projections from the RCP 4.5 models, indicate that if emissions stay near those projected in RCP 4.5, we would expect the effects of forest restoration on mortality to last decades longer than in the RCP 8.5-projected emissions. However, if emissions do follow the trajectory of RCP 8.5, our results indicate that BA reductions alone may not prevent large-scale tree mortality and shifting the species composition to more drought tolerant species may need to be considered (Franklin and Johnson, 2012).

The gridded soils data we used (Hengl et al., 2017) likely introduced error into the model projections because they overestimated the soil depth compared to locally collected soils data from US Forest Service. However, the over-estimated depths led to higher SWA and therefore, provided conservative estimates of mortality due to drought. Our mortality predictions from the USFS soils data showed overall higher mortality but a similar pattern across scenarios and a similar reduction in mortality due to BA reduction (Fig. A.2).

Modeling studies that predict current and future drought mortality based strictly on climate factors are likely to overestimate the extent and severity of drought in western dry forests because they do not account for the modifying influence of forest structure or landscape patterns (McDowell et al., 2016; Williams et al., 2013). This is likely a critical omission because BA increased dramatically across many western dry forests due to fire suppression (Covington and Moore, 1994; Fulé et al., 1997; Hagmann et al., 2021), and contemporary restoration projects aim to increase the pace and scale of forest restoration. 4FRI is only one restoration project in the Collaborative Forest Landscape Restoration Program (CFLRP), which has completed fuel reduction treatments on 3.8 million ha across the western USA, and there are other programs in the region (Initiative, 2019; South Yuba River Citizens League, 2019). The results of our work indicate that thinning may have the potential to reduce mortality across all these landscapes in which significant density reduction is planned. Many dry forests are at risk from tree die-offs from drought and insects, but this study shows that accelerating forest restoration that reduces tree density can limit the risk of tree loss. Reducing tree mortality into mid-century will allow for additional time to understand and mitigate the underlying causes of climate change and reduce the effects of forest loss.

#### Declaration of Competing Interest

The authors declare that they have no known competing financial interests or personal relationships that could have appeared to influence the work reported in this paper.

#### Acknowledgements

We would like to thank the US Forest Service for providing the unpublished 4FRI data used in this project. JBB and CMA were supported by the USGS North Central Climate Adaptation Science Center. Any use of trade, firm, or product name is for descriptive purposes only and does not imply endorsement by the U.S. Government.

#### Appendix A. Supplementary material

Supplementary data to this article can be found online at <https://doi.org/10.1016/j.foreco.2022.120088>.

#### References

Adams, H.D., Barron-Gafford, G.A., Minor, R.L., Gardea, A.A., Bentley, L.P., Law, D.J., Breshears, D.D., McDowell, N.G., Huxman, T.E., 2017. Temperature response surfaces for mortality risk of tree species with future drought. *Environ. Res. Lett.* 12 (11), 115014. <https://doi.org/10.1088/1748-9326/aa93be>.

Allen, C.D., Breshears, D.D., 1998. Drought-Induced Shift of a Forest-Woodland Ecotone: Rapid Landscape Response to Climate Variation. *Proc. Natl. Acad. Sci. USA* 95 (25), 14839–14842.

Allen, C.D., Breshears, D.D., McDowell, N.G., 2015. On underestimation of global vulnerability to tree mortality and forest die-off from hotter drought in the Anthropocene. *Ecosphere* 6 (8), art129. <https://doi.org/10.1890/ES15-00203.1>.

Allen, C.D., Macalady, A.K., Chenchoune, H., Bachelet, D., McDowell, N., Vennetier, M., Kitzberger, T., Rigling, A., Breshears, D.D., Hogg, E.H.C., Gonzalez, P., Fensham, R., Zhang, Z., Castro, J., Demidova, N., Lim, J.-H., Allard, G., Running, S.W., Semerci, A., Cobb, N., 2010. A global overview of drought and heat-induced tree mortality reveals emerging climate change risks for forests. *For. Ecol. Manag.* 259 (4), 660–684. <https://doi.org/10.1016/j.foreco.2009.09.001>.

Anderegg, W.R.L., Anderegg, L.D.L., Kerr, K.L., Trugman, A.T., 2019. Widespread drought-induced tree mortality at dry range edges indicates that climate stress exceeds species' compensating mechanisms. *Glob. Change Biol.* 25 (11), 3793–3802. <https://doi.org/10.1111/gcb.14771>.

Banerjee, S., Gelfand, A.E., Finley, A.O., Sang, H., 2008. Gaussian predictive process models for large spatial data sets. *J. R. Stat. Soc. Ser. B Stat. Methodol.* 70, 825–848. <https://doi.org/10.1111/j.1467-9868.2008.00663.x>.

Bentz, B.J., Régnière, J., Fettig, C.J., Hansen, E.M., Hayes, J.L., Hicke, J.A., Kelsey, R.G., Negron, J.F., Seybold, S.J., 2010. Climate Change and Bark Beetles of the Western United States and Canada: Direct and Indirect Effects. *BioScience* 60, 602–613. <https://doi.org/10.1525/bio.2010.60.8.6>.

Bigler, C., Bräker, O.U., Bugmann, H., Dobbertin, M., Rigling, A., 2006. Drought as an Inciting Mortality Factor in Scots Pine Stands of the Valais, Switzerland. *Ecosystems* 9 (3), 330–343. <https://doi.org/10.1007/s10021-005-0126-2>.

Bottero, A., D'Amato, A.W., Palik, B.J., Bradford, J.B., Fraver, S., Battaglia, M.A., Asher, L.A., Bugmann, H., 2017. Density-dependent vulnerability of forest ecosystems to drought. *J. Appl. Ecol.* 54 (6), 1605–1614. <https://doi.org/10.1111/1365-2664.12847>.

Bradford, J.B., Andrews, C.M., Robles, M.D., McCauley, L.A., Woolley, T.J., Marshall, R.M., 2021. Landscape-scale restoration minimizes tree growth vulnerability to 21st century drought in a dry forest. *Ecol. Appl.* 31 (2) <https://doi.org/10.1002/earp.v31.21002/earp.2238>.

Bradford, J.B., Bell, D.M., 2017. A window of opportunity for climate-change adaptation: easing tree mortality by reducing forest basal area. *Front. Ecol. Environ.* 15 (1), 11–17. <https://doi.org/10.1002/fee.1445>.

Bradford, J.B., Schlaepfer, D.R., Lauenroth, W.K., 2014. Ecohydrology of adjacent sagebrush and lodgepole pine ecosystems: the consequences of climate change and disturbance. *Ecosystems* 17 (4), 590–605. <https://doi.org/10.1007/s10021-013-9745-1>.

Bradford, J.B., Shriner, R.K., Robles, M.D., McCauley, L.A., Woolley, T.J., Andrews, C.A., Crimmins, M., Bell, D.M., 2022. Tree mortality response to drought-density interactions suggests opportunities to enhance drought resistance. *J. Appl. Ecol.* 59 (2), 549–559.

Breshears, D.D., Carroll, C.J.W., Redmond, M.D., Wion, A.P., Allen, C.D., Cobb, N.S., Meneses, N., Field, J.P., Wilson, L.A., Law, D.J., McCabe, L.M., Newell-Bauer, O., 2018. A Dirty Dozen Ways to Die: Metrics and Modifiers of Mortality Driven by Drought and Warming for a Tree Species. *Front. For. Glob. Change* 1, 10 pp. <https://doi.org/10.3389/fgc.2018.00004>.

Breshears, D.D., Cobb, N.S., Rich, P.M., Price, K.P., Allen, C.D., Balice, R.G., Romme, W.H., Kastens, J.H., Floyd, M.L., Belnap, J., Anderson, J.J., Myers, O.B., Meyer, C.W., 2005. Regional vegetation die-off in response to global-change-type drought. *Proc. Natl. Acad. Sci. USA* 102 (42), 15144–15148. <https://doi.org/10.1073/pnas.0505734102>.

Breshears, D.D., López-Hoffman, L., Graumlich, L.J., 2011. When Ecosystem Services Crash: Preparing for Big, Fast, Patchy Climate Change. *AMBIO* 40 (3), 256–263. <https://doi.org/10.1007/s13280-010-0106-4>.

Briley, L., Dougherty, R., Wells, K., Hercula, T., Notaro, M., Rood, R., Andresen, J., Marsik, F., Prosperi, A., Jorns, J., Channel, K., Hutchinson, S., Kemp, C., Gates, O. (Eds.), 2021. A Practitioners Guide to Climate Model Scenarios. Great Lakes Integrated Sciences and Assessments (GLISA), Ann Arbor, Michigan.

Choat, B., Jansen, S., Brodribb, T.J., Cochard, H., Delzon, S., Bhaskar, R., Bucci, S.J., Feild, T.S., Gleason, S.M., Hacke, U.G., Jacobsen, A.L., Lens, F., Maherli, H., Martínez-Vilalta, J., Mayr, S., Mencuccini, M., Mitchell, P.J., Nardini, A., Pittermann, J., Pratt, R.B., Sperry, J.S., Westoby, M., Wright, I.J., Zanne, A.E., 2012. Global convergence in the vulnerability of forests to drought. *Nature* 491 (7426), 752–755. <https://doi.org/10.1038/nature11688>.

Covington, W.W., Moore, M.M., 1994. Southwestern ponderosa forest structure: changes since Euro-American settlement. *J. For.* 92, 39–47.

D'Amato, A.W., Bradford, J.B., Fraver, S., Palik, B.J., 2013. Effects of thinning on drought vulnerability and climate response in north temperate forest ecosystems. *Ecol. Appl.* 23 (8), 1735–1742. <https://doi.org/10.1890/13-0677.1>.

D'Amato, A.W., Jokela, E.J., O'Hara, K.L., Long, J.N., 2017. Silviculture in the United States: An Amazing Period of Change over the Past 30 Years. *J. For.* 116, 55–67. <https://doi.org/10.5849/JOF-2016-035>.

Das, A., Battles, J., Stephenson, N.L., van Mantgem, P.J., 2011. The contribution of competition to tree mortality in old-growth coniferous forests. *For. Ecol. Manag.* 261 (7), 1203–1213. <https://doi.org/10.1016/j.foreco.2010.12.035>.

Dennison, P.E., Brewer, S.C., Arnold, J.D., Moritz, M.A., 2014. Large wildfire trends in the western United States, 1984–2011. *Geophys Res Lett* 41 (8), 2928–2933.

Dickerson-Lange, S.E., Mitchell, R., 2014. Modeling the effects of climate change projections on streamflow in the Nooksack River basin, Northwest Washington. *Hydrocl. Process.* 28 (20), 5236–5250. <https://doi.org/10.1002/hyp.10012>.

Dillon, G.K., Holden, Z.A., Morgan, P., Crimmins, M.A., Heyerdahl, E.K., Luce, C.H., 2011. Both topography and climate affected forest and woodland burn severity in two regions of the western US, 1984 to 2006. *Ecosphere* 2 (12), art130. <https://doi.org/10.1890/ES11-00271.1>.

Fettig, C.J., Reid, M.L., Bentz, B.J., Sevanto, S., Spittlehouse, D.L., Wang, T., 2013. Changing Climates, Changing Forests: A Western North American Perspective. *J. For.* 111 (3), 214–228. <https://doi.org/10.5849/jof.12-085>.

Flathers, K.N., Kolb, T.E., Bradford, J.B., Waring, K.M., Moser, W.K., 2016. Long-term thinning alters ponderosa pine reproduction in northern Arizona. *For. Ecol. Manag.* 374, 154–165. <https://doi.org/10.1016/j.foreco.2016.04.053>.

Franklin, J.F., Johnson, K.N., 2012. A Restoration Framework for Federal Forests in the Pacific Northwest. *J. For.* 110 (8), 429–439. <https://doi.org/10.5849/jof.10-006>.

Fulé, P.Z., Covington, W.W., Moore, M.M., 1997. Determining reference conditions for ecosystem management of southwestern ponderosa pine forests. *Ecol. Appl.* 7 (3), 895–908.

Ganey, J.L., Vojta, S.C., 2011. Tree mortality in drought-stressed mixed-conifer and ponderosa pine forests, Arizona. USA. *For. Ecol. Manag.* 261 (1), 162–168. <https://doi.org/10.1016/j.foreco.2010.09.048>.

elman, A., Carlin, J.B., Stern, H.S., Dunson, D.B., Vehtari, A., Rubin, D.B., 2013. Chapter 7. Evaluating, comparing, and expanding models. In: *Bayesian Data Analysis*. CRC Press Boca Raton, FL, pp. 165–196.

Gealon, K.E., Bradford, J.B., Bottero, A., D'Amato, A.W., Fraver, S., Palik, B.J., Battaglia, M.A., Iverson, L., Kenefic, L., Kern, C.C., 2017. Competition amplifies drought stress in forests across broad climatic and compositional gradients. *Ecosphere* 8 (7). <https://doi.org/10.1002/ecs2.2017.8.issue-710.1002/ecs2.1849>.

Guarín, A., Taylor, A.H., 2005. Drought triggered tree mortality in mixed conifer forests in Yosemite National Park, California. USA. *For. Ecol. Manag.* 218 (1–3), 229–244. <https://doi.org/10.1016/j.foreco.2005.07.014>.

Hagmann, R.K., Hessburg, P.F., Prichard, S.J., Povak, N.A., Brown, P.M., Fulé, P.Z., Keane, R.E., Knapp, E.E., Lydersen, J.M., Metlen, K.L., Reilly, M.J., Sánchez Meador, A.J., Stephens, S.L., Stevens, J.T., Taylor, A.H., Yocom, L.L., Battaglia, M.A., Churchill, D.J., Daniels, L.D., Falk, D.A., Henson, P., Johnston, J.D., Krawchuk, M.A., Levine, C.R., Meigs, G.W., Merschel, A.G., North, M.P., Safford, H.D., Swetnam, T.W., Waltz, A.E.M., 2021. Evidence for widespread changes in the structure, composition, and fire regimes of western North American forests. *Ecol. Appl.* 31 (8) <https://doi.org/10.1002/earp.v31.810.1002/earp.2431>.

Hamlet, A.F., Salathé, E.P., Carrasco, P., 2010. Statistical downscaling techniques for global climate model simulations of temperature and precipitation with application to water resources planning studies. In: Final Report for the Columbia Basin Climate Change Scenarios Project. Climate Impacts Group, Center for Science in the Earth System, Joint Institute for the Study of the Atmosphere and Ocean. University of Washington, Seattle, Washington, USA, p. 28.

Heinrichs, S., Schmidt, W., 2009. Short-term effects of selection and clear cutting on the shrub and herb layer vegetation during the conversion of even-aged Norway spruce stands into mixed stands. *For. Ecol. Manag.* 258 (5), 667–678. <https://doi.org/10.1016/j.foreco.2009.04.037>.

Hengl, T., Mendes de Jesus, J., Heuvelink, G.B.M., Ruiperez Gonzalez, M., Kilibarda, M., Blagotić, A., Shangguan, W., Wright, M.N., Geng, X., Bauer-Marschallinger, B., Guevara, M.A., Vargas, R., MacMillan, R.A., Batjes, N.H., Leenaars, J.G.B., Ribeiro, E., Wheeler, I., Mantel, S., Kempen, B., Bond-Lamberty, B., 2017. SoilGrids250m: Global gridded soil information based on machine learning. *PLOS ONE* 12 (2), e0169748.

Hessburg, P.F., Miller, C.L., Parks, S.A., Povak, N.A., Taylor, A.H., Higuera, P.E., Prichard, S.J., North, M.P., Collins, B.M., Hurteau, M.D., Larson, A.J., Allen, C.D., Stephens, S.L., Rivera-Huerta, H., Stevens-Rummant, C.S., Daniels, L.D., Gedalof, Z., Gray, R.W., Kane, V.R., Churchill, D.J., Hagmann, R.K., Spies, T.A., Cansler, C.A., Belote, R.T., Véblen, T.T., Battaglia, M.A., Hoffman, C., Skinner, C.N., Safford, H.D., Salter, R.B., 2019. Climate, Environment, and Disturbance History Govern Resilience of Western North American Forests. *Front. Ecol. Evol.* 7, 239. <https://doi.org/10.3389/fevo.2019.00239>.

Hurteau, M.D., Bradford, J.B., Fulé, P.Z., Taylor, A.H., Martin, K.L., 2014. Climate change, fire management, and ecological services in the southwestern US. *For. Ecol. Manag.* 327, 280–289. <https://doi.org/10.1016/j.foreco.2013.08.007>.

Jenkins, J.C., Chojnacky, D.C., Heath, L.S., Birdsey, R.A., 2003. National-scale biomass estimators for United States tree species. *For. Sci.* 49, 12–35.

Knutti, R., Sedláček, J., 2013. Robustness and uncertainties in the new CMIP5 climate model projections. *Nat. Clim. Change* 3 (4), 369–373.

Kolb, T.E., Holmberg, K.M., Wagner, M.R., Stone, J.E., 1998. Regulation of ponderosa pine foliar physiology and insect resistance mechanisms by basal area treatments. *Tree Physiol.* 18 (6), 375–381.

Linares, J.C., Camarero, J.J., Carreira, J.A., 2009. Interacting effects of changes in climate and forest cover on mortality and growth of the southernmost European fir forests. *Glob. Ecol. Biogeogr.* 18, 485–497. <https://doi.org/10.1111/j.1466-8238.2009.00465.x>.

Livneh, B., Rosenberg, E.A., Lin, C., Nijssen, B., Mishra, V., Andreadis, K.M., Maurer, E.P., Lettenmaier, D.P., 2013. A long-term hydrologically based dataset of land surface fluxes and states for the conterminous United States: Update and extensions. *J. Clim.* 26 (23), 9384–9392. <https://doi.org/10.1175/JCLI-D-12-00508.1>.

Luo, Y., Chen, H.Y., 2013. Observations from old forests underestimate climate change effects on tree mortality. *Nat. Commun.* 4, 1–6.

Luo, Y., Chen, H.Y.H., 2011. Competition, species interaction and ageing control tree mortality in boreal forests. *J. Ecol.* 99 (6), 1470–1480.

Mantero, G., Morresi, D., Marzano, R., Motta, R., Mladenoff, D.J., Garbarino, M., 2020. The influence of land abandonment on forest disturbance regimes: a global review. *Landscape Ecol.* 35 (12), 2723–2744. <https://doi.org/10.1007/s10980-020-01147-w>.

Maurer, E.P., Brekke, L., Pruitt, T., Duffy, P.B., 2007. Fine-resolution climate projections enhance regional climate change impact studies. *Eos* 88, 504. 10.1029/2007EO470006.

McCauley, L.A., Robles, M.D., Woolley, T., Marshall, R.M., Kretschun, A., Gori, D.F., 2019. Large-scale forest restoration stabilizes carbon under climate change in Southwest United States. *Ecol. Appl.* 29 (8) <https://doi.org/10.1002/earp.v29.810.1002/earp.1979>.

McDowell, N.G., Adams, H.D., Bailey, J.D., Hess, M., Kolb, T.E., 2006. Homeostatic maintenance of ponderosa pine gas exchange in response to stand density changes. *Ecol. Appl.* 16 (3), 1164–1182.

McDowell, N.G., Ryan, M.G., Zeppel, M.J., Tissue, D.T., 2013. Improving our knowledge of drought-induced forest mortality through experiments, observations, and modeling. *New Phytol.* 200, 289–293.

Raffa, K.F., Autkema, B.H., Bentz, B.J., Carroll, A.L., Hicke, J.A., Turner, M.G., Romme, W.H., 2008. Cross-scale Drivers of Natural Disturbances Prone to Anthropogenic Amplification: The Dynamics of Bark Beetle Eruptions. *BioScience* 58, 501–517. <https://doi.org/10.1641/B580607>.

Restaino, C., Young, D.J.N., Estes, B., Gross, S., Wuenschel, A., Meyer, M., Safford, H., 2019. Forest structure and climate mediate drought-induced tree mortality in forests of the Sierra Nevada, USA. *Ecol. Appl.* 29, 14. <https://doi.org/10.1002/earp.1902e01902>.

Reynolds, R.T., Meador, A.J.S., Youtz, J.A., Nicolet, T., Matonis, M.S., Jackson, P.L., DeLorenzo, D.G., Graves, A.D., 2013. Restoring composition and structure in Southwestern frequent-fire forests: A science-based framework for improving ecosystem resiliency (No. Gen. Tech. Rep. RMRS-GTR-310). U.S. Department of Agriculture, Forest Service, Rocky Mountain Research Station, Fort Collins, CO.

Robles, M.D., Marshall, R.M., O'Donnell, F., Smith, E.B., Haney, J.A., Gori, D.F., Jones, J.A., 2014. Effects of climate variability and accelerated forest thinning on watershed-scale runoff in Southwestern USA ponderosa pine forests. *PLoS ONE* 9 (10), e111092.

Rocky Mountain Restoration Initiative, 2019. Restoring Southwest Colorado [WWW Document]. URL <https://rmri2019.files.wordpress.com/2020/09/7351a-southwest-project-information-sheet-updated.pdf>.

Ruiz-Benito, P., Lines, E.R., Gómez-Aparicio, L., Zavala, M.A., Coomes, D.A., Hector, A., 2013. Patterns and Drivers of Tree Mortality in Iberian Forests: Climatic Effects Are Modified by Competition. *PLOS ONE* 8 (2), e56843.

Rupp, D.E., Abatzoglou, J.T., Hegewisch, K.C., Mote, P.W., 2013. Evaluation of CMIP5 20th century climate simulations for the Pacific Northwest USA. *J. Geophys. Res. Atmospheres* 118 (19), 10,884–10,906. <https://doi.org/10.1002/jgrd.50843>.

Schlaepfer, D.R., Andrews, C.M., 2018. rSFSW2: Simulation Framework for SOILWAT2. R package version 3.0.0.

Schlaepfer, D.R., Murphy, R., 2018. rSOILWAT2: An Ecohydrological Ecosystem-Scale Water Balance Simulation Model.

Seager, R., Vecchi, G.A., 2010. Greenhouse warming and the 21st century hydroclimate of southwestern North America. *Proc. Natl. Acad. Sci.* 107 (50), 21277–21282. <https://doi.org/10.1073/pnas.0910856107>.

Shriver, R.K., Yackulic, C.B., Bell, D.M., Bradford, J.B., 2021. Quantifying the demographic vulnerabilities of dry woodlands to climate and competition using rangewide monitoring data. *Ecology* 102 (8). <https://doi.org/10.1002/ecy.v102.810.1002/ecy.3425>.

Sohn, J.A., Hartig, F., Kohler, M., Huss, J., Bauhus, J., 2016. Heavy and frequent thinning promotes drought adaptation in *Pinus sylvestris* forests. *Ecol. Appl.* 26 (7), 2190–2205. <https://doi.org/10.1002/earp.1373>.

South Yuba River Citizens League, 2019. North Yuba Forest Partnership [WWW Document]. URL <https://yubariver.org/n-yuba-forest-partnership/>.

Stan Development Team, 2020. Stan Modeling Language Users Guide and Reference Manual.

Taylor, A.H., 2000. Fire regimes and forest changes in mid and upper montane forests of the southern Cascades, Lassen Volcanic National Park, California. USA. *J. Biogeogr.* 27 (1), 87–104.

Taylor, A.H., Skinner, C.N., 2003. Spatial patterns and controls on historical fire regimes and forest structure in the Klamath Mountains. *Ecol. Appl.* 13 (3), 704–719.

Taylor, K.E., Stouffer, R.J., Meehl, G.A., 2012. An overview of CMIP5 and the experiment design. *Bull. Am. Meteorol. Soc.* 93, 485–498.

Tohver, I.M., Hamlet, A.F., Lee, S.-Y., 2014. Impacts of 21st-Century Climate Change on Hydrologic Extremes in the Pacific Northwest Region of North America. *JAWRA J. Am. Water Resour. Assoc.* 50 (6), 1461–1476. <https://doi.org/10.1111/jawr.12199>.

U.S. Department of Agriculture, Forest Service, 2013. Draft Environmental Impact Statement for the Four-Forest Restoration Initiative (No. MB-R3-04-19). U.S. Forest Service, Flagstaff AZ.

U.S. Department of Agriculture, Forest Service, 1995. Terrestrial ecosystem survey of the Coconino National Forest. U.S. Department of Agriculture, Forest Service, Southwestern Region.

U.S. Department of Agriculture, Forest Service, 1991. Terrestrial ecosystem survey of the Kaibab National Forest. U.S. Department of Agriculture, Forest Service, Southwestern Region.

USDA, Forest Service, 2020. Collaborative Forest Landscape Restoration Program 10-year Report to Congress. USDA Forest Service.

van Mantgem, P.J., Nesmith, J.C.B., Keifer, M.B., Knapp, E.E., Flint, A., Flint, L., Penuelas, J., 2013. Climatic stress increases forest fire severity across the western United States. *Ecol. Lett.* 16 (9), 1151–1156. <https://doi.org/10.1111/ele.12151>.

van Mantgem, P.J., Stephenson, N.L., Byrne, J.C., Daniels, L.D., Franklin, J.F., Fulé, P.Z., Harmon, M.E., Larson, A.J., Smith, J.M., Taylor, A.H., Veblen, T.T., 2009. Widespread Increase of Tree Mortality Rates in the Western United States. *Science* 323 (5913), 521–524.

McDowell, N.G., Williams, A.P., Xu, C., Pockman, W.T., Dickman, L.T., Sevanto, S., Pangle, R., Limousin, J., Plaut, J., Mackay, D.S., Ogee, J., Domec, J.C., Allen, C.D., Fisher, R.A., Jiang, X., Muss, J.D., Breshears, D.D., Rauscher, S.A., Koven, C., 2016. Multi-scale predictions of massive conifer mortality due to chronic temperature rise. *Nat. Clim. Change* 6 (3), 295–300. <https://doi.org/10.1038/nclimate2873>.

Williams, A.P., Allen, C.D., Macalady, A.K., Griffin, D., Woodhouse, C.A., Meko, D.M., Swetnam, T.W., Rauscher, S.A., Seager, R., Grissino-Mayer, H.D., Dean, J.S., Cook, E.R., Gangodagamage, C., Cai, M., McDowell, N.G., 2013. Temperature as a potent driver of regional forest drought stress and tree mortality. *Nat. Clim. Change* 3 (3), 292–297. <https://doi.org/10.1038/nclimate1693>.

Williams, A.P., Allen, C.D., Millar, C.I., Swetnam, T.W., Michaelsen, J., Still, C.J., Leavitt, S.W., 2010. Forest responses to increasing aridity and warmth in the southwestern United States. *Proc. Natl. Acad. Sci.* 107 (50), 21289–21294. <https://doi.org/10.1073/pnas.0914211107>.

Williams, D.W., Liebhold, A.M., 2002. Climate change and the outbreak ranges of two North American bark beetles. *Bark Beetles Fuels Fire Bibliogr.* 4 (2), 87–99. <https://doi.org/10.1046/j.1461-9563.2002.00124.x>.

Young, D.J.N., Stevens, J.T., Earles, J.M., Moore, J., Ellis, A., Jirka, A.L., Latimer, A.M., Lloret, F., 2017. Long-term climate and competition explain forest mortality patterns under extreme drought. *Ecol. Lett.* 20 (1), 78–86. <https://doi.org/10.1111/ele.12711>.

Zhao, M., Running, S.W., 2010. Drought-Induced Reduction in Global Terrestrial Net Primary Production from 2000 Through 2009. *Science* 329 (5994), 940–943.